Characteristics of 100 nm-Dot Array of Vertically Aligned Carbon Nanotube Field Emitters Fabricated by DC Plasma Enhanced Chemical Vapor Deposition

Takafumi MATSUDA, Jun SATO[1], Akihisa OGINO, and Masaaki NAGATSU

Graduate School of Science and Technology, Shizuoka University, 3-5-1 Johoku, Naka-ku, Hamamatsu, 432-8561, Japan

[1] Graduate School of Engineering, Shizuoka University, 3-5-1 Johoku, Naka-ku, Hamamatsu, 432-8561, Japan

(Received: 1 September 2008 / Accepted: 17 October 2008)

Vertically aligned carbon nanotube field emitters with 100 nm-dot array structure were fabricated using dc plasma enhanced chemical vapor deposition, where dot catalysts were patterned by electron beam lithography. In order to optimize the growth condition of VACNTs, the morphologies of CNTs were investigated by changing gas ratio between NH_3 and C_2H_2 gases. It was found that morphology of CNTs changed from bamboo-like to hollow type structure by decreasing a C_2H_2 ratio from 25 % to less than 15%. Optical emission spectroscopy measurement was also carried out at various NH_3/C_2H_2 gas ratios, where emissions of CH and C_2 radicals increased with increasing a C_2H_2 gas ratio while H radicals remain almost constant. A bamboo-like CNT formation might be resulted from the excessive carbon supply at higher C_2H_2 gas ratios. It was found from the field emission measurements that turn-on voltages were reduced from 1.9 V/μm for bamboo-like CNTs to 1.2 V/μm for hollow type CNTs.

Keywords: vertically aligned carbon nanotubes, field emission, plasma enhanced chemical vapor deposition, nano-sized dot array catalyst.

1. Introduction

Field emission from carbon nanotubes (CNTs) was firstly reported in 1995 [1]. They have extraordinary features such as high aspect ratio, electrical conductivity, or mechanical strength and make it possible to realize field emission applications such as field emission display (FED) [2], X- ray tubes [3] and so on. Advantages of CNTs as field emitters are the low turn-on voltage and large current density [4], compared to other carbon related materials. Recently, ion gauge using CNT field emitters have been also developed [5, 6]. Generally, Fowler-Nordheim (F-N) equation is employed to evaluate the field emission characteristics, which include the field enhancement factor and work function. For reduction of work function, low work function materials such as Cs [7], MgO [8] or BaO/SrO [9] are deposited on the surface of CNTs, which lead to the improvement of field emission characteristics. On the other hand, controls of diameter, alignment or density of CNTs have been carried out to better the field enhancement factor.

It is well known that diameters of CNTs are determined from the thickness of initial catalyst film, that is, diameter increases with catalyst film thickness [10-12]. In our previous work, we proposed to use graphene-layer encapsulated Ni nanoparticles as catalyst to grow the narrower multi-walled CNTs (MWCNTs) [13]. MWCNTs have diameter ranging from 2 to 5 nm, which are narrower CNTs compared with CNTs grown from Ni film.

Another important factor is the alignment of CNTs. Some research groups reported that growth direction of CNTs was controlled by applied electric fields and that electric field of order of 0.1~1.0 V/μm is necessary to align the CNTs [14-17]. In our previous work, vertically aligned CNTs (VACNTs) were grown on Si substrate using thermal CVD under the applied electric fields [18]. In the experiment, vertical alignment of CNTs might be explained by the electrostatic force acting on the negatively charged tip of CNTs under a negative electric field. The other factor is density of CNTs. It is well known that electric field shielding effect is occurred in high density CNTs, which deteriorates the field emission characteristics. In numerical calculations, the highest value of electric field enhancement factor β was obtained when the dot interval was roughly two times the length of CNTs [19]. Electric field shielding effects have been investigated by changing the dot intervals, where the experimental result showed the similar tendency as the calculation [20].

In this study, with dc-PECVD method, VACNTs were grown on 100 nm-dot array catalyst dots, which were fabricated by electron beam lithography technique, in order to develop the nano-sized VACNTs field emitters. Flow

author's e-mail:tmnagat@ipc.shizuoka.ac.jp

rate ratios of NH_3/C_2H_2 gas mixtures were varied to study the CNT morphology and field emission characteristics.

2. Experimental details

For preparing substrates, a Cr thin film was deposited on Si substrate by the radio frequency magnetron sputtering to form the diffusion barrier layer. After then, Ni thin film was deposited on the substrate as catalyst. Fabrication of nano-sized dot catalyst array was carried out by lift-off process using electron beam lithography.

Figure 1 shows our thermal CVD system with a cylindrical quartz tube, where parallel diode type electrodes with an inter-electrode distance of about 5 mm were inserted in the quartz tube. The substrate was put on the electrode and heated up to 700 ^oC. Pre-treatment using NH_3 gas was carried out for 5 min to activate catalyst surface. After then, DC discharge was ignited by applying voltages between two electrodes and NH_3/C_2H_2 gas mixtures were introduced at the pressure of 400 Pa for 15 min to grow the CNTs. Figure 2 shows the typical field emission type scanning electron microscopy (FE-SEM) image of VACNTs grown on Ni uniformly deposited substrate under the applied voltage of -650 V. In this experiment, we have confirmed the vertical growth of CNTs in higher voltage than -600 V. So applied voltage for plasma ignition is fixed at -650 V. Moreover, gas ratios of NH_3/C_2H_2 were changed from 15 % to 25 % in order to control the CNT morphology while total gas flow rate was kept at 150 sccm.

The surface morphology of CNTs was analyzed using JEOL JSM-6320F FE-SEM and JEOL JEM-2000FXII transmission electron microscope (TEM). Field emission characteristics of CNTs were measured with a parallel diode configuration at a pressure of 10^{-4} Pa. A Kapton sheet with a thickness of 125 μm was used as a spacer.

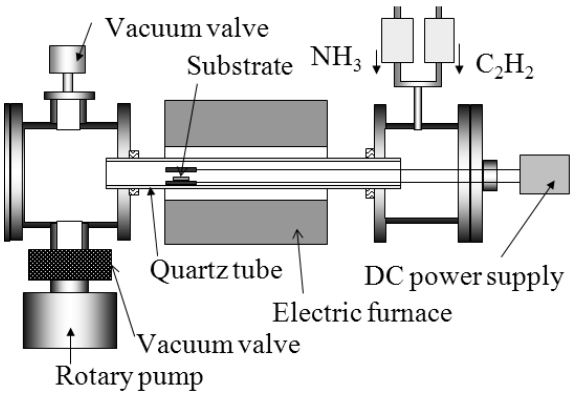

Fig.1 PECVD reactor for VACNT growth

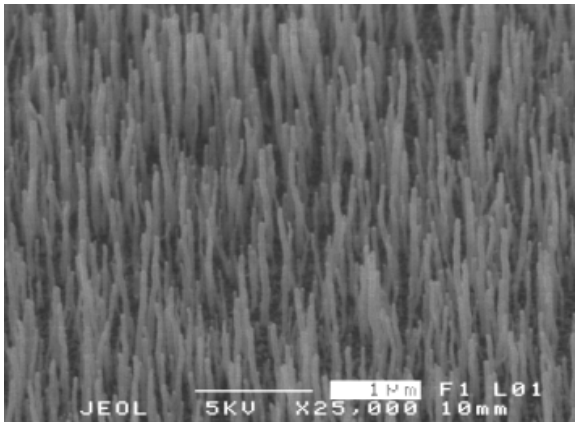

Fig.2 FE-SEM image of VACNTs grown on Ni uniformly deposited Si substrate.

3. Results and discussion

Figure 3 shows the typical FE-SEM image of VACNT field emitters with 100 nm-dot array structure, where C_2H_2 flow rate ratio to NH_3 was 25%. In this work, all the samples are prepared with 100nm dot and 10 μm interval. Single VACNT was grown on each catalyst dot uniformly which have a length of 3.5 μm. As for the morphology, it looks like fiber structure rather than tube, which top and bottom diameter is 70~80 nm and 100~150 nm, respectively. From TEM measurement, we have confirmed the morphology bamboo like structure. Some research groups also fabricated CNT field emitter array [21-23]. In these papers, however, the morphology looks like carbon nanofibers (CNFs) or carbon nanocones (CNCs). Therefore NH_3/C_2H_2 gas flow rate were optimized to grow VACNTs.

Dependency of NH_3/C_2H_2 gas flow rate ratio on the CNT morphology was investigated by changing C_2H_2 gas flow rate ratio to NH_3 from 15 % to 25 % while total gas flow rate was kept at 150 sccm. Figure 4 shows the FE-SEM images of the dependency on the CNT morphology. VACNT was grown on catalyst dot with C_2H_2 ratio of 15%, which diameter is ranging from 60 to 80 nm, as shown in Fig. 4(a). On the other hand, morphology was changed from CNTs to fiber like structure with increasing C_2H_2 ratio from 15% to 25%, as shown in Fig.4. In the case of ratio of 25%, the morphology showed the similar tendency as that of Fig. 3. This result showed the same tendency as the paper reported by Chhowalla et al [11] or Teo et al [22]. At concentration over 50%, VACNT growth cannot keep pace with the amount of carbon extruded the catalyst, which the lateral growth below the catalyst cap

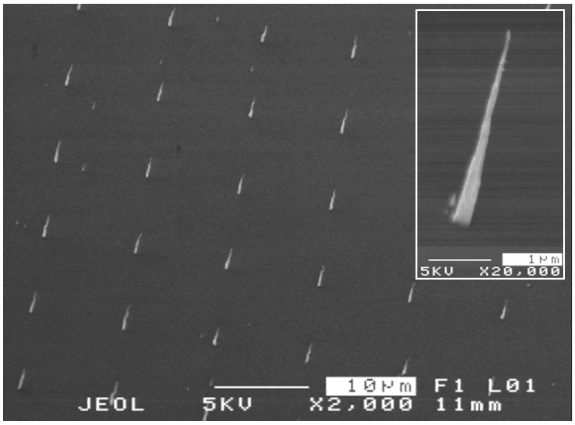

Fig.3 FE-SEM image of VACNTs grown on 100 nm dot array catalysts (dot interval is 10 μm.)

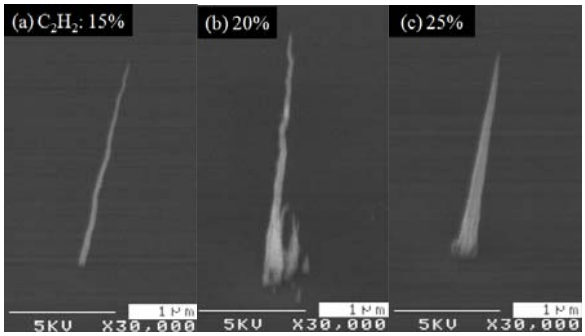

Fig.4 FE-SEM images of VACNT grown on 100 nm dots at different C_2H_2 gas flow rate ratios of (a) 15 %, (b) 20 %, and (c) 25 %.

dominates giving rise to fiber like structures.

TEM analysis was carried out to investigate the structure of CNTs with different NH_3/C_2H_2 gas flow rate ratio. Figure 5 shows TEM images of CNTs grown at C_2H_2 ratio of 15% and 25%. Both samples have catalyst particle at tip which has almost the same diameter, as shown in Fig. 5(a) and (b). On the contrary, focused on the bottom region, CNTs grown at ratio of 25% have larger diameter, as shown in Fig. 5(d), which is in agreement with FE-SEM analysis. In addition, there is a difference in inner tube structure. It is hollow structure at C_2H_2 ratio of 15% while that of C_2H_2 ratio of 25% is bamboo like structure. Cui et al reported that CNTs have bamboo like structure at higher ratio of CH_4 than 50% [24], which showed the similar results with our results.

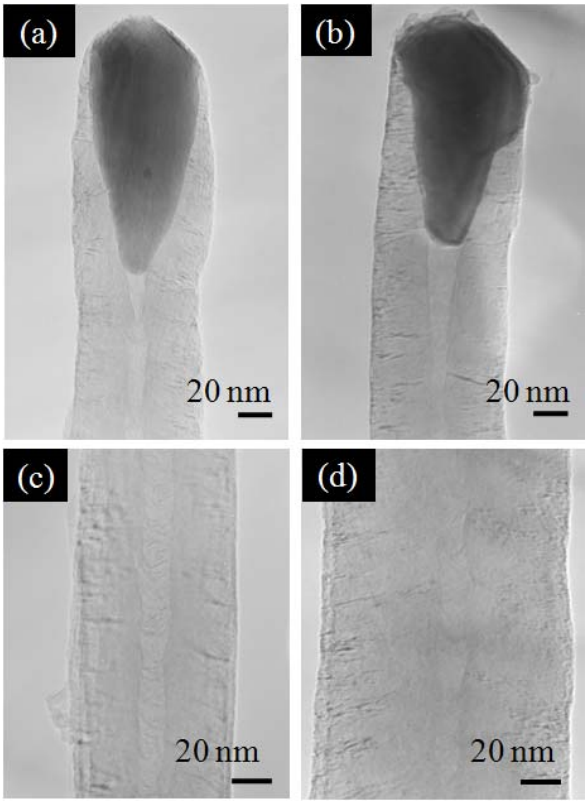

Fig.5 TEM images of VACNT grown on 100 nm-dot of the top region: (a) 15 %, (b) 25 % and the bottom region: (c) 15 %, (d) 25 %.

Optical emission spectroscopy (OES) measurement was carried out to investigate chemical species in NH_3/C_2H_2 plasma. Figures 6 (a) and (b) show the OES spectrum at C_2H_2 ratio of 25%. The chemical species identified mainly in this study include NH at 336 nm, N_2^+ at 358.5 nm, CN at 388 nm, CH at 390 nm, H_δ at 410 nm, CH at 431 nm, H_γ at 434 nm, C_2 at 469 nm, H_β at 486 nm, C_2 at 516.5 nm, H_α at 656.5 nm, and N_2 at 672.6 nm [25-29]. It is noted that an additional peak of N_2 at 672.6 nm was observed in our system, which was different from other reports [25-27]. Figure 6 (c) shows the dependency of C_2H_2 ratios on the relative intensity of H_α, H_β, C_2, and CH radical. The intensity of hydrogen radicals including H_α and H_β remains almost constant, which are considered

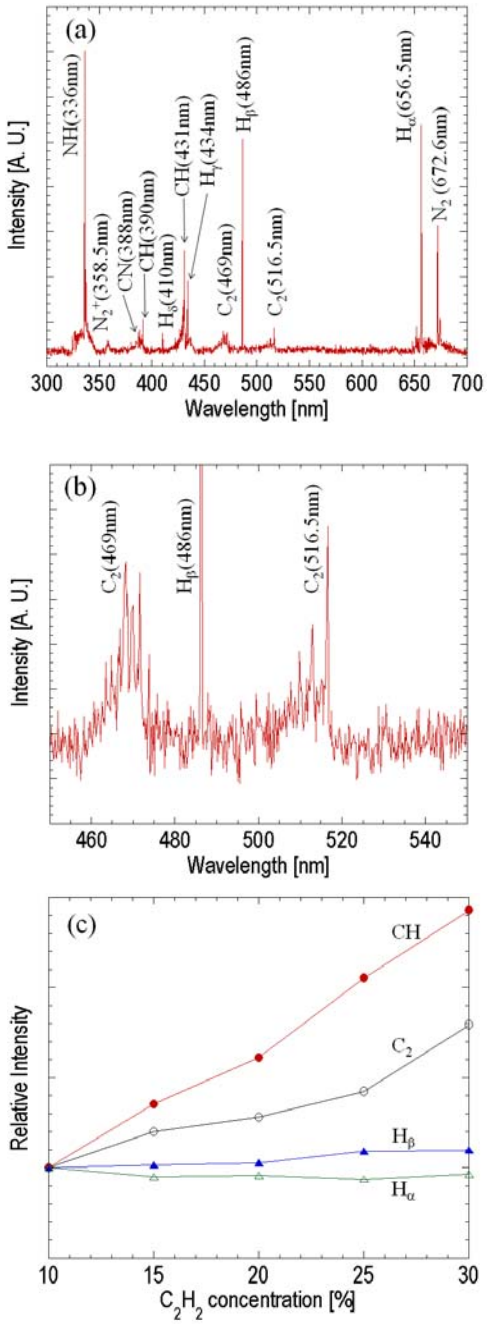

Fig.6 (a) OES spectrum obtained at C_2H_2 ratio of 25 % and (b) C_2 swan bands. Figure (c) shows the relative intensity with different C_2H_2 ratios.

to be etching species. Figure 6(c) suggested that hydrogen radicals might be considered to be generated from NH_3 and C_2H_2. On the other hand, intensity of carbon source radical such as C_2 and CH increased drastically with C_2H_2 gas flow rate. From these results, the CNT morphology was changed from hollow to bamboo like structures as a result of excessive carbon feeding.

Finally, field emission characteristics were measured with VACNTs grown at C_2H_2 ratio of 15% and 25%, as shown in Fig. 7. In this work, electric shielding effect can be negligible because dot interval was twice longer than length of VACNTs [20]. Therefore the morphology effect of individual free-standing CNTs on field emission characteristics can be evaluated. Turn-on voltages of VACNT field emitters grown at C_2H_2 ratio of 15% and 25% are 150 V (1.2 V/μm) and 240 V (1.9 V/μm), respectively. The field emission characteristics were improved by changing the morphology, as shown in Fig. 4. And these results were analyzed by F-N plots, as shown in Fig.7 (b). Here, we can evaluate the value of field enhancement factor β from the extrapolated linear slopes of F-N plots, simply assuming that work function of CNTs is roughly 4.9 eV. β were evaluated to be 2930 and 4720,

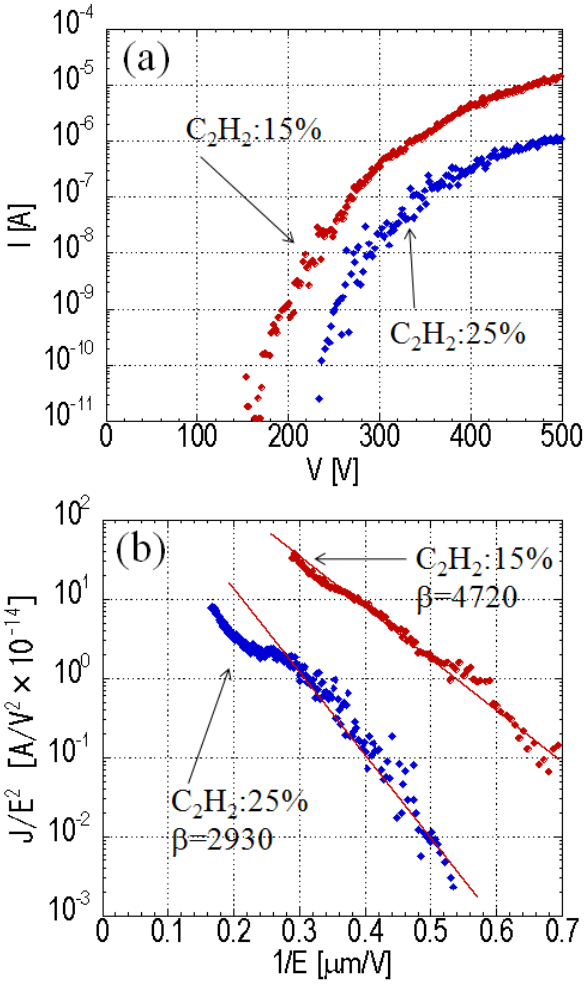

Fig.7 Comparison of (a) field emission characteristics and (b) F-N plots of VACNTs grown at C_2H_2 gas ratios of 15% and 25%.

for VACNT field emitters grown at C_2H_2 gas ratio of 15% and 25%, respectively. Experimental results suggested that the narrower CNTs with a higher aspect ratio might result in lower turn-on voltage due to stronger field enhancement factor than bamboo-like CNTs.

4. Conclusions

100nm-dot array VACNT field emitters were fabricated using dc PECVD, where dot catalysts were patterned by electron beam lithography. Dependency of NH_3/C_2H_2 gas flow rate ratios on CNT morphology was investigated in order to optimize the growth conditions by changing from 15% to 25%. The morphology was transferred from bamboo-like CNTs to hollow structure with decreasing C_2H_2 ratio to less than 15%. And optical emission spectroscopy was performed in various NH_3/C_2H_2 gas ratios, where CH and C_2 radical increased with C_2H_2 ratio with C_2H_2 ratio. On the contrary, H radical remained constant. Bamboo-like CNT formation might be resulted from excessive carbon supply from these experimental results. Field emission characteristics were compared between these samples, which turn-on voltages were reduced from 1.9 V/μm for bamboo-like CNTs to 1.2 V/μm for CNTs with hollow structure. That might be resulted from the improvement of field enhancement factor by controlling the CNT morphology.

Acknowledgements

This work was supported in part by the Grants-in-Aid for Scientific Research and performed under the 21 Century COE Program “Research and Education Center of Nanovision of Science” by the Japan Society for the Promotion of Science. The authors would like to thank Professor M. Tabe and Mr. T. Mizuno of RIE of Shizuoka University for electron beam lithography and Associate Professor K. Murakami of RIE Shizuoka University for FE-SEM analysis and Professor K. Tatsuoka of Shizuoka University for TEM analysis.

References

[1] W. A. de Heer, A. Chatelain, and D. Ugarte, Science **270** 1179 (1995).

[2] Y. Saito, K. Hamaguchi, R. Mizushima, S. Uemura, T. Nagasako, J. Yotani, and T. Shimojo, Appl. Surf. Sci. **146** 305 (1999).

[3] J. Zhang, G. Yang, Y. Cheng, B. Gao, Q. Qiu, Y. Z. Lee, J. P. Lu and O. Zhou, Appl. Phys. Lett. **86** 184104 (2005).

[4] W. Zhu, C. Bower, O. Zhou, G. Kochanski, and S. Jin, Appl. Phys. Lett. **75** 873 (1999).

[5] I. M. Choi, S. Y. Woo, and H. W. Song, Appl. Phys. Lett. **90** 023107 (2007).

[6] C. A. Bower, K. H. Gilchrist, J. R. Piascik, and B. R. Stoner, S. Natarajan, C. B. Parker, S. D. Wolter, and J. T. Glass, Appl. Phys. Lett. **90** 124102 (2007).

[7] A. Wadhawan, R. E. Stallcup II, and J. M. Perez, Appl. Phys. Lett. **78** 108 (2001).
[8] S. Chakrabarti, L. Pan, H. Tanaka, S. Hokushin, and Y. Nakayama, Jpn. J. Appl. Phys. **46** 4364 (2007).
[9] F. Jin, Y. Liu, C. M. Day, and S. A. little, Carbon **45** 587 (2007).
[10] C. Bower, O. Zhou, W. Zhu, D. J. Werder, and S. Jin, Appl. Phys. Lett. **77** 2767 (2000).
[11] M. Chhowalla, K. B. K. Teo, C. Ducati, N. L. Rupesinghe, G. A. J. Amaratunga, A. C. Ferrari, D. Roy, J. Robertson, and W. I. Milne: J. Appl. Phys. **90** 5308 (2001).
[12] Y. Y. Wang, S. Gupta, R. J. Nemanich, Z. J. Liu, and L. C. Qin, J. Appl. Phys. **98** 014312 (2005).
[13] M. Nagatsu, T. Yoshida, M. Mesko, A. Ogino, T. Matsuda, T. Tanaka, H. Tatsuoka, and K. Murakami, Carbon **44** 3336 (2006).
[14] Y. Zhang, A. Chang, J. Cao, Q. Wang, W. Kim, Y. Li, N. Morris, E. Yenilmez, J. Kong, and H. Dai, Appl. Phys. Lett. **79** 3155 (2001).
[15] A. Nojeh, A. Ural, R. F. Pease, and H. Dai, J. Vac. Sci. Technol. B **22** 3421 (2004).
[16] C. Bower, W. Zhu, S. Jin, and O. Zhou, Appl. Phys. Lett. **77** 830 (2000).
[17] V. I. Merkulov, A. V. Melechko, M. A. Guillorn, D. H. Lowndes, and M. L. Simpson, Appl. Phys. Lett. **79** 2970 (2001).
[18] T. Matsuda, M. Mesko, T. Ishikawa, J. Sato, A. Ogino, R. Tamura, and M. Nagatsu, Jpn. J. Appl. Phys. **47** 7436 (2008).
[19] L. Nilsson, O. Groening, C. Emmenegger, O. Kuettel, E. Schaller and L. Schlapbach, Appl. Phys. Lett. **76** 2071 (2000).
[20] T. Matsuda, M. Mesko, A. Ogino, M. Nagatsu, Diam. and Relat. Mater. **17** 772 (2008).
[21] Z. F. Ren, Z. P.Huang, J. G. Wen, J. W. Xu, J. H. Wang, L. E. Calvet, J. Chen, and M.A. Reed, Appl. Phys. Lett. **75** 1086 (1999).
[22] K. B. K. Teo, M. Chhowalla, G. A. J. Amaratunga, W. I. Milne, D. G. Hasko, G. Pirio, P. Legagneux, F. Wyczisk, and D. Pribat, Appl. Phys. Lett. **79** 1534 (2001).
[23] L. R. Baylor, V. I. Merkulov, E. D. Ellis, M. A. Guillorn, D. H. Lowndes, A. V. Melechko, M. L. Simpson, and J. H. Whealton, J. Appl. Phys. **91** 4602 (2002).
[24] H. Cui, O. Zhou, and B. R. Stoner, J. Appl. Phys. **88** 6072 (2000).
[25] T. Y. Lee, J. H. Han, S. H. Choi, J. B. Yoo, C. Y Park, T. Jung, S. Yu, W. K. Yi, I. T. Han, and J. M. Kim, Diam and Relat. Mater. **12** 851 (2003).
[26] S. Hofmann, B. Kleinsorge, C. Ducati, A. C. Ferrari, and J. Robertson, Diam and Relat. Mater. **13** 1171 (2004).
[27] S. H. Lim, H. S. Yoon, J. H. Moon, K. C. Park, and J. Jang, Appl. Phys. Lett. **88** 033114 (2006).
[28] K. Yasui, T. Arayama, S. Okutani, and T. Akahane, Appl. Surf. Sci. **212-213** 619 (2003).
[29] S. K. Srivastava, V. D. Vankar, and V. Kumar, Thin Solid Films **515** 1552 (2006).